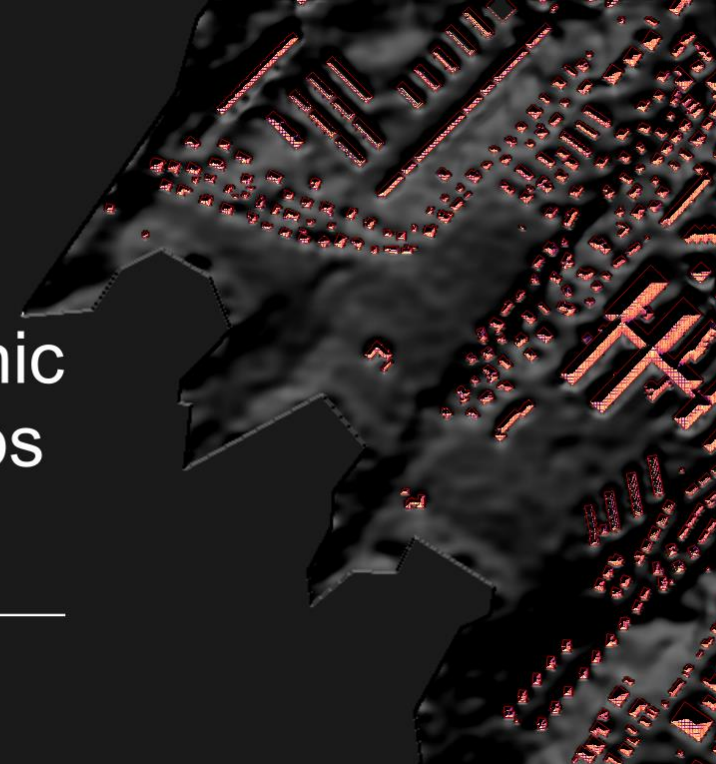


A GIS-base approach to estimate the geographic solar potential of rooftops in Greenland



Aalborg University Copenhagen

MSc Geoinformatics, Institute of Planning



**AALBORG
UNIVERSITY**

Master Thesis

8th January 2021

Paweł Józef Baszanowski

Abstract

Global warming is one of the major problems facing man in the twenty-first century. Scientists are reporting that an uncontrolled rise in Earth's temperature could have devastating consequences for the planet. The main cause of global warming is the greenhouse effect, occurring as a result of emissions of greenhouse gases. Greenhouse gases, mainly carbon dioxide, are produced by burning fossil fuels. One way to reduce greenhouse gas emissions is to replace fossil fuel energy with renewable energy sources. Falling prices and increasing efficiency of photovoltaic panels make the production of electricity from solar energy more accessible and profitable. The aim of this thesis is to calculate the solar roof potential of buildings in Greenland. The data used in this project is publicly available and free, all calculations are made using open-source software. The results show significant spatial and temporal variation of the geographical potential of solar irradiation in Greenland. Mean solar irradiation potential for clear sky conditions, in an average day of the year, based on calculations for all roofs in Greenland equals to 2921 Wh/m²/day.

Keywords: solar irradiation, Greenland, r.sun, ArcticDEM,

Author: Paweł Józef Baszanowski

Supervisor: Prof. Carsten Keßler

Education: MSc in Geoinformatics, Master's program

University: Aalborg University Copenhagen, Denmark

Preface

This Master's Thesis is a summary of my work during the final semester of the Geoinformatics Master's program at Aalborg University. The main purpose of this work is to estimate the solar potential of roofs in Greenland.

The inspiration to apply geoinformatics to solar energy research in arctic and sub-arctic regions comes from my interest in renewable energy sources, which I see as technologies that offer hope for a better future. In 2019, I had the opportunity to do a student internship at the Greenland Institute of Natural Resources in Nuuk. The choice of Greenland as a research area is a natural consequence of the experiences and passion I have for this part of the world.

I would like to express my gratitude to my supervisor, Prof. Carsten Keßler, for the support, enthusiasm, and professional advice during whole period of writing this master thesis. In addition, I would like to thank my family who supported me while writing this work and throughout all my studies.

Definitions and Acronyms

name	acronym
Digital elevation model	DEM
Digital surface model	DSM
Command Line Interface	CLI
Graphic User Interface	GUI
Geographical Resources Analysis Support System	GRASS
Geographic information system	GIS
Photovoltaic Geographical Information System	PVGIS
Gigabyte	GB
Terabyte	TB
Kilowatt-hour	kWh
Megawatt-hour	MWh
Gigawatt-hour	GWh
Watt-hour	Wh
Carbon dioxide	CO₂
Nitrogen oxides	NO_x
Sulfur dioxide	SO₂
United Nations	UN
Random-access memory	RAM
Universal Transverse Mercator coordinate system	UTM
Photovoltaics	PV
Linke turbidity factor	TL

List of Figures

Figure 1 Horizon angles traced along specified number of directions (left), Viewshed calculated for one cell of a DEM (right) (Fu & Rich, 1999, p. 5 and 7)	11
Figure 2 Annual sunmap for 39°N (day intervals half-hour, season intervals one month) (Fu & Rich, 1999, p. 8)	11
Figure 3 Skymap (sectors defined by 16 zenith divisions and 16 azimuth divisions) (Fu & Rich, 1999, p. 9)	12
Figure 4 Buildings footprints.....	16
Figure 5 Greenland - ArcticDEM tile index.....	17
Figure 6 Download tiles - python code.....	18
Figure 7 Unpack tar.gz archives - python code	18
Figure 8 Godthåbsfjord near Narsap Sermia glacier. The image on the left - ArcticDEM, the image on the right - Google Satellite.....	18
Figure 9 Buildings in Nuuk shown with ArcticDEM and the same area without and with the building footprints.....	19
Figure 10 Multi-ring buffer inside building outline.	19
Figure 11 The terraced houses divided into residential risers (A, D). QGIS “dissolve” tool connect multiple polygons into one representing whole building (B). Inner buffers produced from “dissolved” polygons (C) are better representation of the roofs structure than those generated from multiple polygons (E).	20
Figure 12 Measuring the roof angle in Google Street View	21
Figure 13 The angle of the roof slope in relation to the building area – manual classification results .	22
Figure 14 3D model represents elements that add up to the value of the buffer height (the "basenroof" value).....	23
Figure 15 ArcticDEM before (left) and after (right) adding buffer height values from the vector layer.	23
Figure 16 GRASS GIS graphical modeler	26
Figure 17 Monthly sum of solar irradiation and Mean irradiation value for an average day of the month	28
Figure 18 Solar irradiation for an average day in a month in relation to the latitude	28
Figure 19 Greenland mean solar irradiation, potential Yearly sum of solar irradiation.....	29
Figure 20 Solar irradiation in the middle day of the month. Example from Nuuk.	30
Figure 21 Mean solar irradiation in an average day of the year for four different roof slope directions	31
Figure 22 Mean solar irradiation for an average day in a year	32
Figure 23 Yearly sum of solar irradiation per m2	33

List of Tables

Table 1 690 measured roofs grouped by angle range.....	21
Table 2 Solar irradiation values in an average day of the year grouped by roof aspect.....	32
Table 3 Comparison of electrical production from photovoltaic panels in Igaliku with the estimated solar irradiance potential.....	33

Table of Contents

Abstract	1
Preface.....	2
Definitions and Acronyms.....	3
List of Figures.....	4
List of Tables.....	4
Table of Contents	5
1 Introduction.....	6
1.1 Research questions	7
2 Literature review	8
2.1 Potential definition.....	8
2.2 Solar potential modeling.....	9
2.3 Modeling solar irradiation potential on the rooftops.....	13
3 Methodology	15
3.1 Input data	15
3.2 Clear sky global solar irradiation modeling.....	24
4 Results.....	27
4.1 Data validation	33
5 Discussion	35
5.1 Limitations of the input data	36
5.2 Modeling process	37
5.3 Future work	39
6 Conclusion.....	41
Bibliography	42

1 Introduction

Data on the solar potential of roofs can be useful for both public administration and individual users. Gathering information about solar irradiance on all the roofs in Greenland, allows the analysis of the potential at the national, local and the level of individual building. The aim of this master's thesis is to create a database containing the value of potential solar irradiation in watt hours per square meter per day (Wh / m² / day) for every building in the country.

Directing the focus on building roofs when calculating solar irradiation potential has several reasons. Roofs as surfaces elevated above the surrounding area are a good basis for photovoltaic panels. The installation on the housetop reduces the potential shading of neighboring objects, therefore possible losses of electrical production are limited. Panels installed on the roof are difficult to access, which reduces the risk of damage. On the other hand, inaccessibility of the site is an obstacle during cleaning, snow removal or maintenance. Roofs with an appropriate slope provide a natural basis, which reduces installation costs, moreover, the installation located above the building is always close to the power line, therefore the costs of connecting to the electricity grid is reduced. Finally, implementing these technologies on the roof uses the space that already has an existing land-use. Roof based system does not require the new space, which can be used for other purposes. Greenland, with over 2 million square kilometers, is the largest island and at the same time the least populated country in the world. Consequently, the last of the arguments is less relevant than in densely populated countries.

The solar potential of roofs in Greenland was previously unexplored. There are no detailed maps that consider local conditions resulting from the topography or urban development. General information about solar potential of the country can be found on maps covering the whole world, although even those are often lacking data for areas at high latitudes.

Roughly 79% of the Greenland surface is covered by the ice sheet. 56,081 residents (Greenland, 2020) is living in more than 23,000 households (Lading, 2015) which are located in more than 60 settlements scattered along the east and west

coasts of the island. Due to hardware and time constraints, it would be impossible to create accurate solar irradiation maps for the entire area of Greenland within the time frame of this thesis. Because the country characteristics and the above-mentioned limitations, the insolation potential is calculated only in built-up areas and the analyzes are limited to the outlines of buildings. Narrowing of the area of interest allows the calculation of the geographical solar irradiation potential for all the roofs on the island within the limited time frame of this thesis.

Originally, it was planned to create solar potential maps based on detailed digital surface model generated from the geodata collected with lidar during the 2019 air mission (GIM, 2020). Unfortunately, detailed surface models of Greenlandic cities were not released until the completion of this thesis. It became necessary to use other available data sources. Main data source used in this work is ArcticDEM, a terrain model based on data generated from the panchromatic bands of the WorldView satellites¹. This digital elevation model with resolution of 2 meters covers whole territory of Greenland.

1.1 Research questions

Following research questions were formulated aiming at using open-source technologies and data for estimation of solar irradiation potential of rooftops in Greenland.

- **How does the solar potential of rooftops in Greenland vary spatially and temporally, and to what degree can this information be extracted from solar irradiation estimations based on open-source data?**
- **How can two meter resolution open-source DEM be adapted for modeling solar irradiation potential with a particular focus on rooftops?**

¹ <https://worldview.earthdata.nasa.gov/>

2 Literature review

This chapter review the existing literature on solar energy. The first part describes the definitions use in hierarchical perspective often used to estimate the potential of renewable energy sources. The following section describes progress in solar energy potential estimation. Examples of different ways of estimating solar potential on roofs depending on the scale of the analyzed area will be presented at the end.

2.1 Potential definition

The hierarchical perspective on the potential estimation of renewable energy sources has been described by Hoogwijk (2004). In her work she has defined five different categories of solar potential:

The theoretical potential results from the theoretical limit of the primary resource, which is yearly sum of solar energy irradiated on the Earth's surface.

The geographical potential is dependent on the conditions in the analyzed location. Elevation, surface reflectance, slope, aspect, and shadowing effect of neighboring objects are factors influencing the solar energy potential of a given area, and its spatial diversity on the Earth's surface.

The technological possibility of converting energy from the primary energy source into secondary energy determines the technological potential. The technological potential equals to geographical potential reduced by losses due to the conversion process of solar energy to electrical energy. (Hoogwijk, 2004)

The economic potential is derived from the technological potential and is based on the economic competitiveness of solar energy in relation to alternative energy sources. It is a technical potential restricted to electricity that can be produced in a cost-effective manner.

The last defined by Hoogwijk (2004) is the implementation potential. It results from the maximum economic potential that can be used at a given time frame, considering the adversities and indications. Barriers to the implementation of

photovoltaic systems can be the available capital, aesthetic considerations, or administrative restrictions. The implementation potential may be greater than economic, e.g., when the need to care for air quality is more important than costs. However, it cannot exceed the technological potential, limited by the efficiency of individual components of the photovoltaic system.

This master's thesis focuses on determining the geographic potential for solar radiation on the roofs of Greenland, does not analyze specific technological solutions or the possible costs of their implementation. Therefore, the technological, economic or implementation potential are not considered.

2.2 Solar potential modeling

Attempts to describe the characteristics of solar energy, its interaction with the atmosphere and the earth's surface date back to the early twentieth century. Solar irradiation computational models are based on empirical and meteorological observations of solar radiation, and consider factors such as atmospheric transparency, latitude, albedo coefficient, surface angle and slope, and the shading effect caused by surrounding objects.

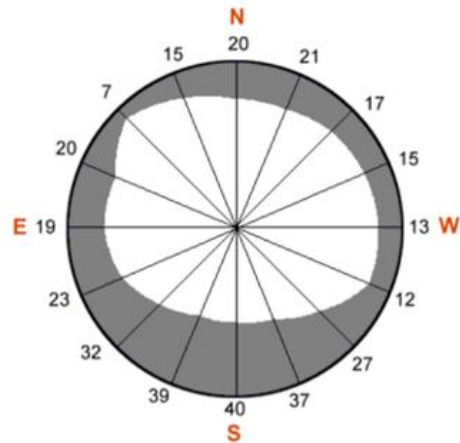
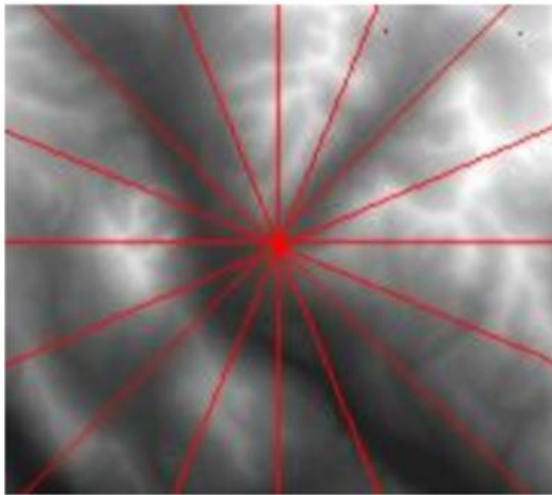
The energy of solar radiation on the horizontal plane outside the Earth's atmosphere is estimated at 1.367 W / m^2 , after reaching the Earth's surface, this value drops to 342 W / m^2 . (Scharmer & Grief, 2000) This value is further modified depending on the latitude, day of the year or time of day. The amount of solar energy reaching the Earth's surface depends on the path it must travel through the atmosphere as well as on the characteristics of atmospheric particles. Molecules in the atmosphere scatter, reflect and absorb part of the solar radiation. Characteristics of specific locations on Earth surface, such as latitude, slope, aspect, height, reflectance impact solar irradiance values. (Scharmer & Grief, 2000)

Direct, diffuse and reflected irradiation are components of global solar irradiation. Direct irradiation is the part of solar radiation which, undisturbed by obstacles such as atmospheric particles, clouds, or trees, reaches the Earth's surface directly. Direct irradiation is the largest component of global solar irradiation. Solar

radiation, which is scattered by the particles of the atmosphere on its way to the earth's surface, is called diffuse radiation. It reaches a given point from all directions. Diffuse radiation increases its share to global radiation when the atmosphere is more turbid, e.g., on days with full cloud cover. Reflected irradiation is smallest part of global radiation, it reach the point where irradiation is measured after being reflected from another surface. (Kumar, Skidmore, & Knowles, 1997)

The 1980s and 1990s are a period when technological advances greatly contributed to accelerating the development of solar irradiation modeling. It happened due to three factors. The first was the increase in the performance of computers allowing the processing of bigger amounts of data, the second was the creation of Geographic Information Systems (GIS), and the last one was the development of the digital surface model (DSM). (Kumar, Skidmore, & Knowles, 1997).

Two models used to estimate insolation potential have gained popularity. It is, used in this thesis r.sun, which is based on GRASS and QGIS open-source platforms, and Solar Analyst based on commercial ArcGIS by ESRI, distributed with the Spatial Analyst extension. Solar Analyst is developed from 1993 first as SOLARFLUX by Hetrick et al.(Hetrick, Rich, & Weiss, 1993), then perfected by Kumar et al. (1997) and adopted in its current version at the beginning of the twentieth century by Fu and Rich (1999). R.sun was developed by Hofierka and Suri (2004) and then implemented to the GRASS GIS platform by Netler and Mitasova (2008). Hofierka and Zolha (2012) introduced the r.sun-based v.sun module, which can be used 3D vector objects for modeling instead of DSM or DEM. Both models use DEM as basic input data. The main difference is in the way in which shadow effects from adjacent objects are accounted for. As described by Fu and Rich (1999), viewsheds (Figure 1) are computed for each DEM cell. It is the angular distribution of sky obstruction. They compare it to watching the horizon from ground level through a fisheye lens. Viewshed is computed in several directions around the cell. A horizontal angle is calculated for each of the directions. The more analyzed directions, the more detailed the picture of sky obstruction. For not computed directions, horizon angles are interpolated.



The resulting viewshed for a location represents which sky directions are visible and which are obscured. Numbers represent the calculated horizon angles.

Figure 1 Horizon angles traced along specified number of directions (left), Viewshed calculated for one cell of a DEM (right) (Fu & Rich, 1999, p. 5 and 7)

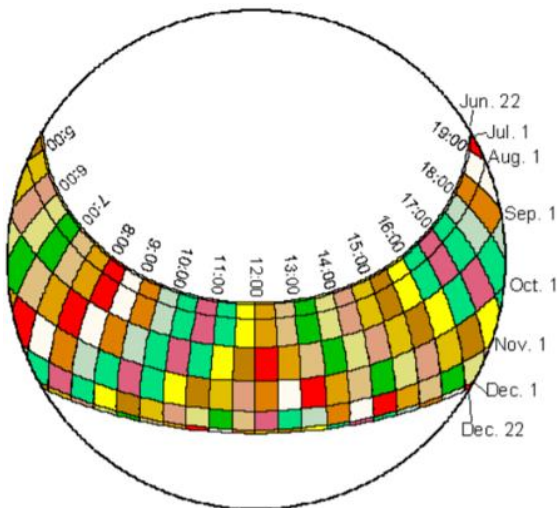


Figure 2 Annual sunmap for 39°N (day intervals half-hour, season intervals one month) (Fu & Rich, 1999, p. 8)

Another element of the Solar Analysis model is the sunmap (Figure 2). Sunmap provides information on the amount of direct solar radiation emitted from each direction of the sky. Sunmap specifies suntracks on a specific day and time for a given latitude. It is created in the same hemispherical projection as for the viewshed. The position of the sun (zenith and azimuth) is projected on two-dimensional grid. Two sunmaps are generated, one for the period from December 22 to January 22, and another

for the second part of the year. The sunmap is divided into sectors defined by the suntracks and segmented according to the set intervals for the day and season (for example: the day is divided into half-hour intervals, the season is divided into months). (Fu & Rich, 1999)

Skymaps are created to account for diffuse radiation in the Solar Analyst model. Solar radiation scattered by atmospheric particles can reach a given point on the surface from any direction, so the skymaps cover the entire surface of the sky. The sky is divided into sectors determined by zenith and azimuth divisions. The zenith and

azimuth for each sector's centroids are determined. The number of sectors must be adequate to provide the desired sky detail (e.g., the skymap in Figure 3 is derived from dividing the sky into 16 azimuth divisions and 16 zenith divisions). (Fu & Rich, 1999)

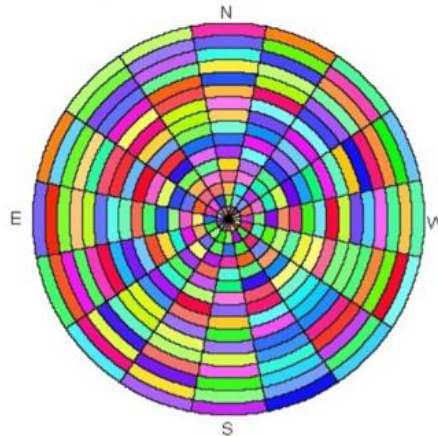


Figure 3 Skymap (sectors defined by 16 zenith divisions and 16 azimuth divisions) (Fu & Rich, 1999, p. 9)

Reflected radiation, as a very small fraction of global radiation, is not considered in the Solar Analyst model.

One of the Solar Analyst variables allows to set the proportion of diffused radiation in the global radiation. Proper setting of this proportion allows to imitate the sky conditions, such as cloudiness or other atmospheric phenomena. Another settable parameter in this model is transmissivity. It is the ratio of the amount of energy reaching the Earth's surface to the amount of energy absorbed by the upper parts of the atmosphere. The lower the transmissivity value, the more solar radiation is absorbed and diffused by the atmosphere.

The R.sun model calculates direct, diffuse, reflected or global irradiation for a specific hour or the sum of solar radiation for a set time frame. The model developed by Suri and Hofierka (2004) is based on the equations performed for the European Solar Radiation Atlas (ESRA) (Scharmer & Grief, 2000). Suri and Hofierka (2004) argue that the main advantage of r.sun is the possibility of using radiation attenuator variables in the form of raster maps, which are better representation of conditions for large areas than the single variables used in, for example, Solar Analyst.

R.sun takes into account the shading resulting from the height of the horizon surrounding the insolation measurement point. For this purpose, it calculates the height of the horizon for a given number of directions. The calculation of the horizon maps is as follows. In the designated direction, the line is led at a minimum angle, if

the end of the line meets the terrain, the angle is raised to avoid the obstacle exactly above it. The process continues until the line reaches a height that avoids all points in its path or when it reaches the border of the region. A raster map is created for each of the directions for which the horizon height is determined. The number of calculated directions affects the precision of the modeled horizon as well as the time of the process. When calculating the horizon for large areas, equations consider the curvature of the earth.

2.3 Modeling solar irradiation potential on the rooftops

Modeling of the solar potential of rooftops takes various forms and depends mainly on the scale of the research area and the available input data. Analyses in country or continental scale often use a statistical approach. Analyses at the level of individual cities apply more precise input data in the such as detailed terrain models and vector models of buildings.

An example of a statistical approach can be found in the study by Suri et al. (2005). They use PVGIS² database with a resolution of 1km to estimate the energy potential for most European countries. To define the size of built-up areas, they used CORINE³ land cover class 11 (urban fabric) with a resolution of 100m. The results are presented as averages for Eurostat administrative boundaries at NUTS 3 level⁴.

The method of estimating the solar potential of rooftops at the level of a single city is presented in the work of Hofierka and Kaňuk (2009). They used a 1m resolution terrain model as input. Based on the available maps, they vectorized the outlines of the buildings. During the field work, they collected data on the building morphology properties and solar related roof attributes. These data served as input data for the r.sun model. Based on calculations, they determined that the technological potential at could cover 2/3 of the electricity demand in the analyzed city of Bardejov.

An example of a large-scale detailed modeling of solar radiation can be Project Sunroof⁵ developed by Google (2017). This project estimates the technological potential of roofs for individual addresses in most cities in US, Europe and Japan and

² <https://ec.europa.eu/jrc/en/pvgis>

³ <https://land.copernicus.eu/pan-european/corine-land-cover>

⁴ <https://ec.europa.eu/eurostat/web/gisco/geodata/reference-data/administrative-units-statistical-units/nuts>

⁵ <https://www.google.com/get/sunroof>

major cities in South America, China and South Africa (state for 2020). The calculations are based on 3D models of buildings. The shading effect of trees, adjacent buildings, and roof elements within a radius of 100-150 meters is taken into account. The deep learning model is used to correctly define roof boundaries based on satellite images, e.g. by recognizing and excluding trees and other obstacles. The results are presented on a web portal where users can estimate the number of solar panels needed to cover the current energy demand for a given address.

3 Methodology

This chapter describe the methodology used to estimate potential of solar irradiation on the rooftops in Greenland. Firstly, the input data will be presented and preparation of it explained. Second part of this section focus on the modeling process.

The following master's thesis was created within 4 months, from September 2020 to the beginning of January 2021. The author's laptop - Lenovo IdeaPad 700 was used to perform the calculations. It is equipped with the Intel Core i5-6300HQ 2.30GHz processor, 12 GB of RAM, two hard drives with total of 1200 GB capacity of which around 1 TB was available. The hardware resources proved to be sufficient to estimate the solar irradiation potential of all roofs in Greenland.

3.1 Input data

One of the two main data input is the vector dataset that contains 2D buildings footprints. Polygons with the buildings footprints are part of Asiaq's Greenland Survey Basemap. The Basemap is the term for highly accurate database covering all towns and settlements in Greenland. Data in the Basemap has a horizontal accuracy of 0.05 meters and vertical accuracy of 0.1 meters. It is based on data from vertical aerial photography, as well as on data from variety of sources like reports from public authorities and businesses. According to the supplier, the data can be used for tasks related to nature conservation, land planning and management, infrastructure planning, transport and logistics, tourism applications as well as environmental, natural, climate, culture, and history research. According to its metadata "The Basemap is updated according to an established updating strategy with a recurring rotation." (Asiaq Greenland Survey). Metadata does not specify exact date of the last update. List of 17 cities and 57 settlements⁶, where the Basemap is updated was created in June 2016 and updated in January 2018. All data is in the local UTM zones.

⁶ https://www.asiaq-greenlandsurvey.gl/wp-content/uploads/2018/05/Asiaq_Lokalitetsliste_2018.pdf

The data is open and can be downloaded at no cost from Asiaq's portal⁷. Data for this thesis is download in Esri shapefile format.

Shapefile with building footprints contains 19567 objects that have total area of 2.725.170 m² or 2,725km². Attribute table contains information about building number, location, creation date, last edit date, building type, shape length or shape area. Polygons with area smaller than 1.65m², and polygons that represents roofs over footpaths in Nuuk were removed. That reduced the total area of remain buildings to 2.723.540 m² or 2,724 km².

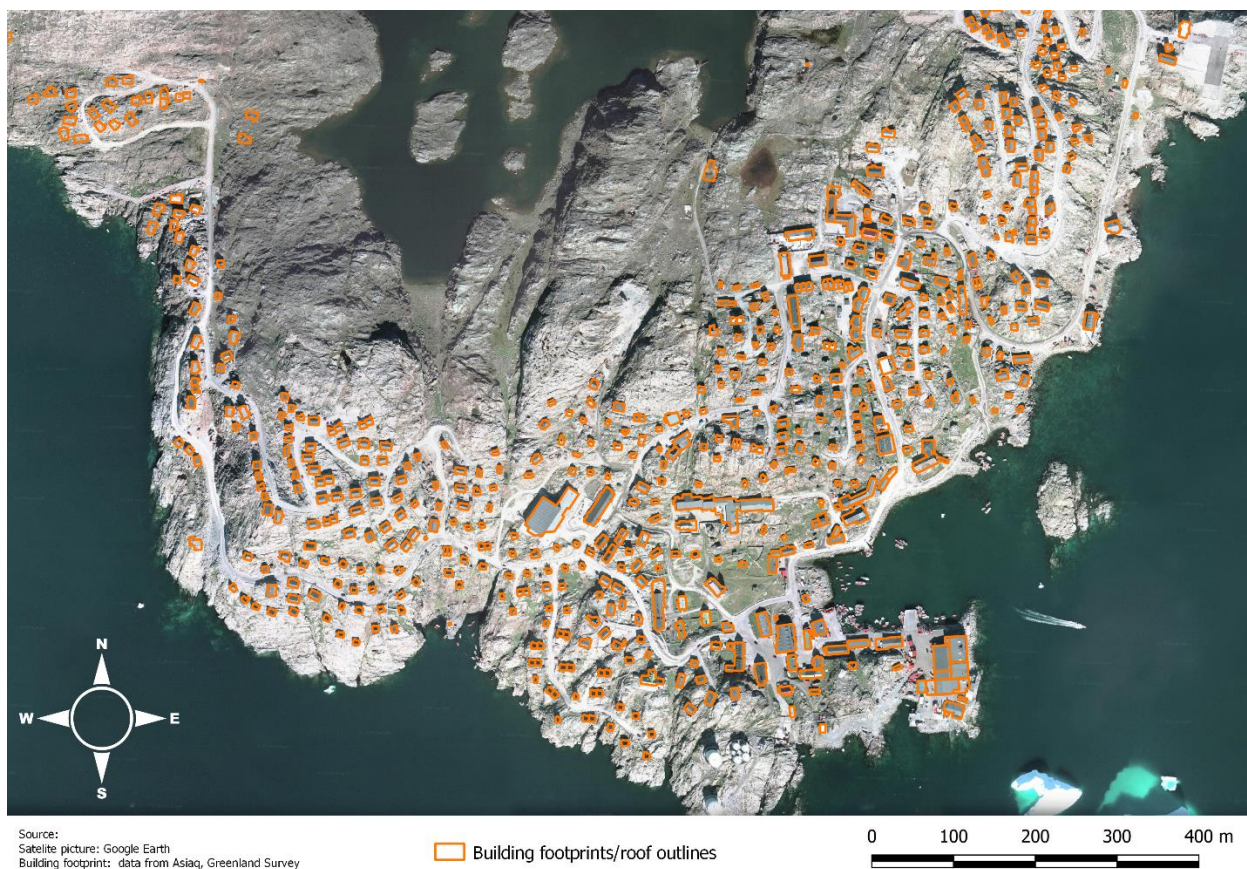


Figure 4 Buildings footprints

Second main data sources used in this thesis is a Digital Elevation Model (DEM) produced by Polar Geospatial Center founded by the US National Geospatial-intelligence Agency and a team led by the US National Science Foundation⁸.

⁷ <https://kortforsyning.asiaq.gl/gb.html>

⁸ <https://www.nsf.gov/>

Discussed terrain model is known as the ArcticDEM⁹ and is based on stereoscopic imagery from DigitalGlobe's Worldview-1, 2 and 3 satellites. Data provided by the satellites is processed by the University of Illinois's Blue Water supercomputer using Surface Extraction from TIN-based Searchspace Minimization (SETSM) software designed at the Ohio State University by M.J. Noh and Ian Howat. The ArcticDEM domain includes all land north of 60°N, entire state of Alaska, Kamchatka Peninsula in the Russian Federation, and entire territory of Greenland. Data is available as single strip DEM files which correspond to the coverage of the original stereoscopic imagery provided by the satellites, or mosaic DEM raster files blended from multiple strips which covers larger areas. Mosaic tiles are based on the best quality strips and are provided in 50 km x 50 km sub-tiles in 32-bit GeoTIFF format. Spatial resolution of ArcticDEM equals 2 meters. Elevation units are meters and are reference to WGS84 ellipsoid. All tiles of ArcticDEM are in Sea Ice Polar Stereographic North projection and referenced to WGS84 horizontal datum (EPSG:3413). (Morin, et al., 2016)

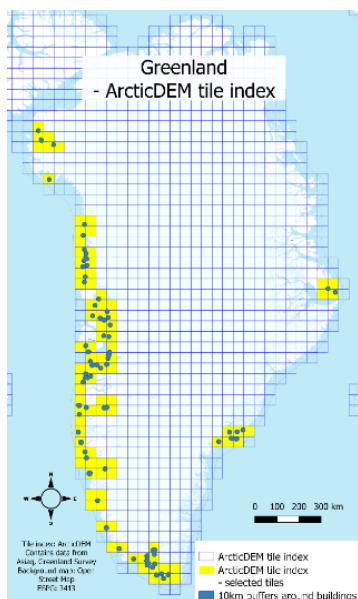


Figure 5 Greenland - ArcticDEM tile index

Following steps are made to download the ArcticDEM raster files. 10km buffers around buildings polygons are generated and merged into one object. QGIS “Select by location” tool is applied to intersect ArcticDEM tile index with the 10km buffers. 92 tiles were selected from the tile index (Figure 5). Settlements are concentrated on the coast of the island, and most of the selected tiles are located in the west of Greenland, with only a few in the east. The central ice-covered part of the island is not included in this thesis.

File URL address of selected tiles are exported into csv file. In next step python code is applied to automate downloading process (Figure 6).

⁹ <https://www.pgc.umn.edu/data/arcticdem/>

```

1 import csv
2 import webbrowser
3 from time import sleep
4
5 f = open('list_of_tiles_to_download_buffered10km.csv')
6 csv_f = csv.reader(f)
7 for row in csv_f:
8     webbrowser.open(row[0])
9     sleep(120) # Time in seconds
10 f.close()

```

Figure 6 Download tiles - python code

To unpack downloaded Arctic DEM tiles stored in tar.gz format another python script is used (Figure 7).

```

1 import tarfile
2
3 if fname.endswith("tar.gz"):
4     tar = tarfile.open(fname, "r:gz")
5     tar.extractall()
6     tar.close()
7 elif fname.endswith("tar"):
8     tar = tarfile.open(fname, "r:")
9     tar.extractall()
10    tar.close()

```

Figure 7 Unpack tar.gz archives - python code

The size of the downloaded DEM files after unpacking equals 160GB. Figure 8 shows the comparison of the ArcticDEM to the satellite picture. 2-meter resolution terrain model accurately maps the steep cliffs, hills, rock formations, little lakes, or the structure of the glacier's surface.



Figure 8 Godthåbsfjord near Narsap Sermia glacier. The image on the left - ArcticDEM, the image on the right - Google Satellite.

The example from Nuuk (Figure 9) shows the ArcticDEM in the urban area. In an image without a vector layer, it is difficult to see the shapes of the buildings. Shapes of the houses in the example are blurry. The 2-meter resolution, which reflects well the geomorphological diversity, is not precise enough to model roof surfaces. In the next part of this section, we will outline the efforts to achieve a more faithful representation of buildings by ArcticDEM.

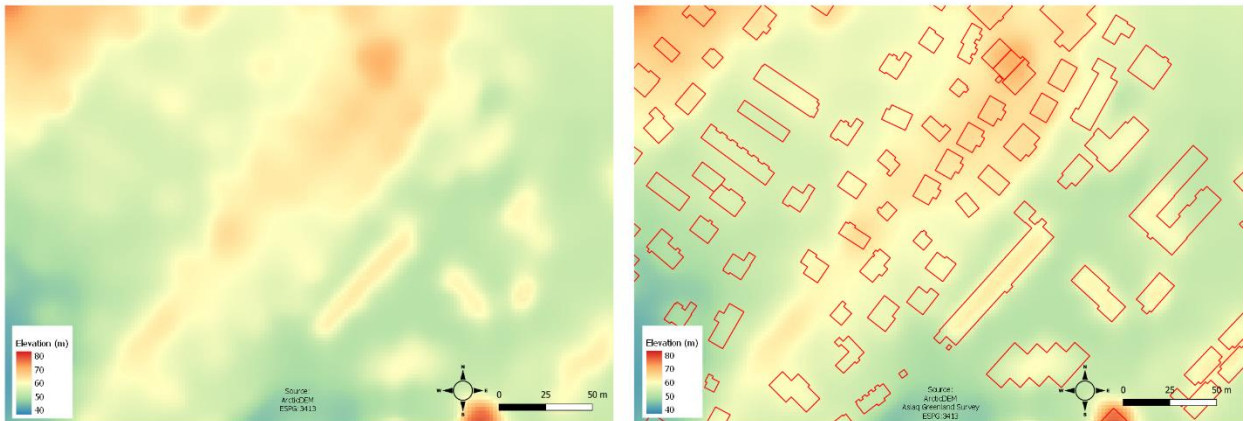


Figure 9 Buildings in Nuuk shown with ArcticDEM and the same area without and with the building footprints.

To modify the ArcticDEM to improve building detail, buildings footprints from the vector layer was used. For purpose of this project, it is assumed that the outlines of the buildings correspond to the outlines of the roofs. To create simplified roof models, multi-ring buffer (constant distance) function in Qgis3 is applied. The outlines of buildings are segmented to form a series of internal buffers. The distance between buffers is set to -0.5m . The negative value of the distance between the rings determined the direction of the buffers towards the center of the polygon. (Figure 10)

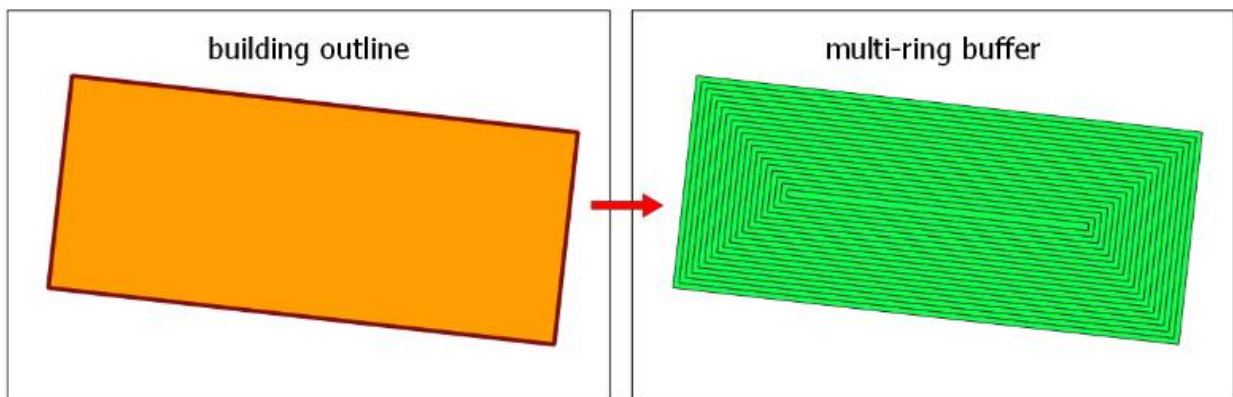


Figure 10 Multi-ring buffer inside building outline.

Most buildings in the Asiaq shapefile are delineated by the single polygons. However, polygons representing some constructions, mainly terraced or semi-detached houses, are divided into smaller parts which are corresponding to the single addresses. QGIS tool “dissolve” is applied to connect those separated segments into one shape that matches the outline of the roof. The use of orthophotos as a base layer during the analysis of segmented buildings outlines made it possible to assess whether the structure of a roof is continuous, and thus which polygons should be connected using the aforementioned tool.(Figure 11)

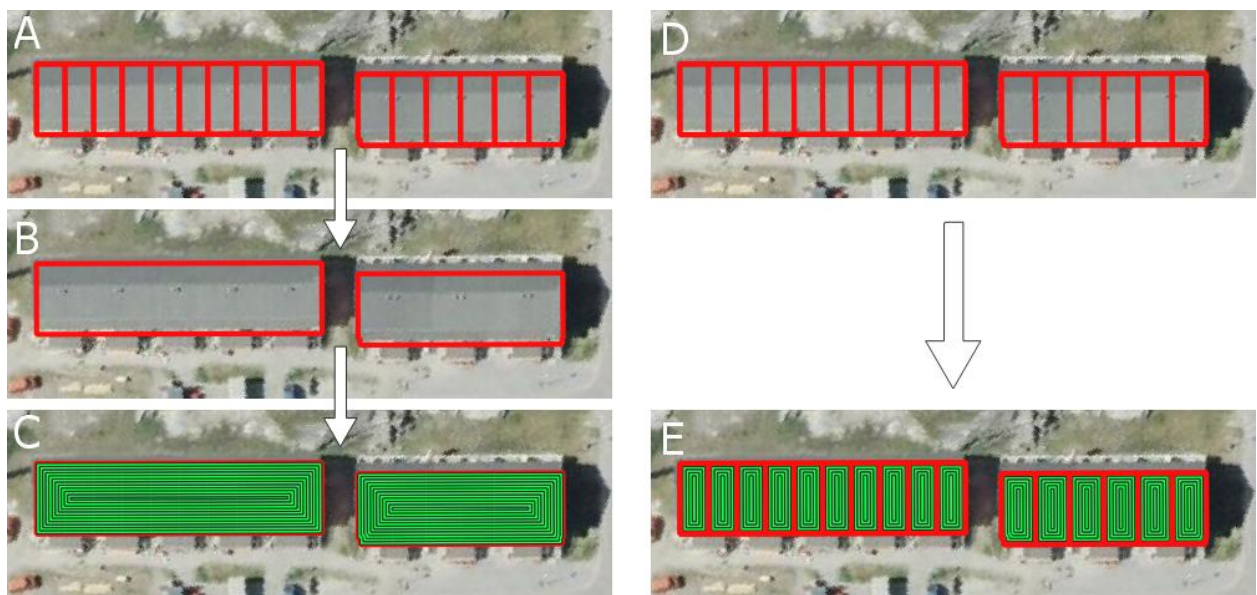


Figure 11 The terraced houses divided into residential risers (A, D). QGIS “dissolve” tool connect multiple polygons into one representing whole building (B). Inner buffers produced from “dissolved” polygons (C) are better representation of the roofs structure than those generated from multiple polygons (E).

Asiaq’s shapefile does not contain any data about roof type, roof angle or buildings height. To classify buildings by the roof pitch, satellite images and Google Street View are used. Google Street View is a function of Google Maps¹⁰ and Google Earth¹¹ that allows to have a panoramic view of the selected location from the perspective of the street. The first step is to add a new column called "Roof_angle" to the vector layer containing the outlines of the buildings. Buildings from the vector layer are localized in Google Earth, then the angle of the roof is measured from the level of Google Street View. The "Protractor" plug-in for the Chrome web browser is used to determine the angular value. (Figure 12)

¹⁰ <https://www.google.com/maps/>

¹¹ <https://www.google.com/intl/en/earth/>



Figure 12 Measuring the roof angle in Google Street View

Roof angle of 690 buildings were measured with above method. The measured constructions were divided into 4 groups. Group 0 includes buildings with flat roofs, group 1 buildings with a roof slope from 1 to 9 degrees, group 2 from 10 to 40 degrees, and group 3 includes buildings with a roof slope greater than 40 degrees (Table 1).

Table 1 690 measured roofs grouped by angle range

	Angle range	Mean angle measured	Number of buildings measured	Mean shape area (m ²)	Model angle
Group 0	0	0	82	1483	0
Group 1	1-9	5	4	623	5
Group 2	10-40	21,5	240	394	25
Group 3	41-45	44,8	364	66	45

The analysis of the measurements shows that the buildings with the smallest area (in the case of Greenland these are mostly traditional single-family houses), are mostly covered by roofs with the greatest slope (up to 45 degrees) (Figure 13). The larger the building area, the smaller the roof slope. Bigger apartment blocks are often covered with roofs with a slope of between 20 and 30 degrees. In the buildings with the largest area on the island, such as warehouses, airports, industrial or public buildings, the roof pitch is the smallest.

Considering the above assumptions - buildings which were not classified manually are divided as follows:

- Buildings with shape area < 200m² - roof angle = 45°
- Buildings with shape area >200 m² <1000 m² - roof angle =25°
- Buildings with shape area>1000 m² - roof angle= 5°
- Buildings with flat roofs, easy to recognize on the orthophotos, have been classified manually.

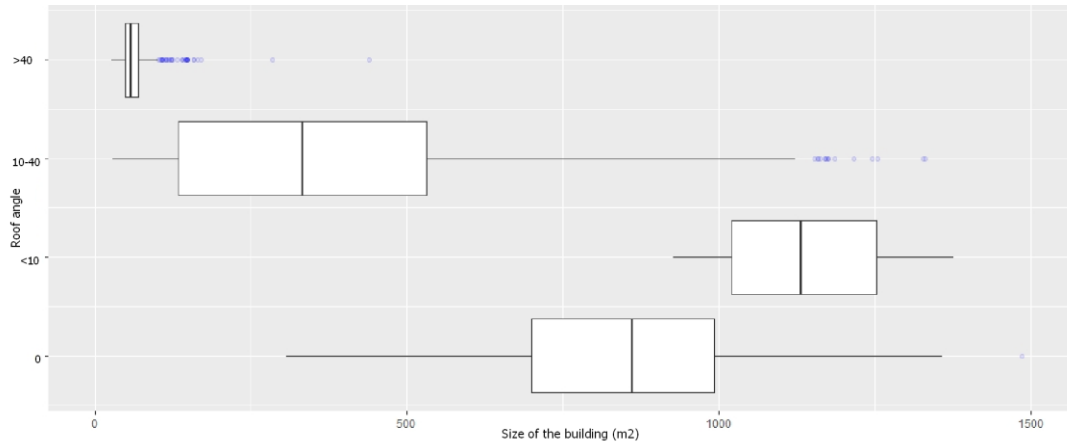


Figure 13 The angle of the roof slope in relation to the building area – manual classification results

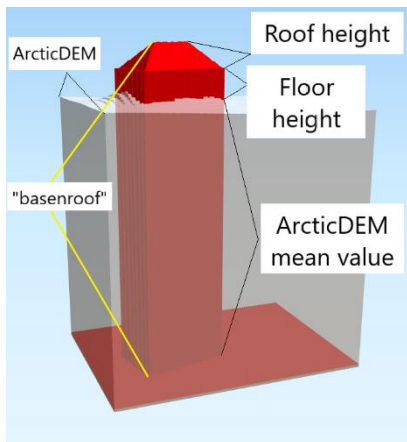
Base on the analysis of satellite images and Google Street View, the general assumption that buildings with an area smaller than 175m² have one story below the roof line is made. Buildings over 175m² are classified as two-story buildings. There are exceptions to this rule, however limited timeframe in which this master's thesis is produced does not allowed for more precise classification of all buildings. The floor height is set at 4.5 m.

QGIS zonal statistics tool is applied to determine the mean altitude value for each building in the vector layer. Altitude value for the polygons is set base on mean cell value of the ArcticDEM within the outline of the building.

Each of the buffers generated inside the outline of the building is attributed with the height value, which increases the closer to the center of the polygon. Height value for each of the following buffers depends on the roof slope. Knowing that the width of the buffers is 50cm and that each buffer has the "ringid" value that increase by 1 from the outside to the center of the building, the roof height values are calculated as follows:

- Buffers in buildings with roof slope of 45 degrees: (ringid) * 0,5m
- Buffers in buildings with roof slope of 25 degrees: (ringid) * 0,23315m

- Buffers in buildings with roof slope of 5 degrees: $(\text{ringid}) * 0,04374\text{m}$
- Buffers in buildings with roof slope of 0 degrees: $(\text{ringid}) * 0$



Sum of the mean altitude value, the height of the floors and the roof height is set as the elevation above sea level of each buffer, and added as a new column in the buffers layer attribute table named "basenroof". (Figure 14)

Figure 14 3D model represents elements that add up to the value of the buffer height (the "basenroof" value)

In the next step, the buffer height values from the vector layer are plotted on the raster terrain model. For more precise mapping of roofs shapes from the vector layer, fragments of the ArcticDEM raster layers containing cities and settlements are exported in an increased resolution of 0.5 x 0.5 m into new files. To

plot the shapes of the buffers on the ArcticDEM raster layer, the "rasterize (overwrite with attribute)" QGIS tool is applied. Values from "basenroof" field are burn in the cells of the 0.5m resolution ArcticDEM. Effect of transformation ArcticDEM by applying the height values of the roof buffers is shown on Figure 15.

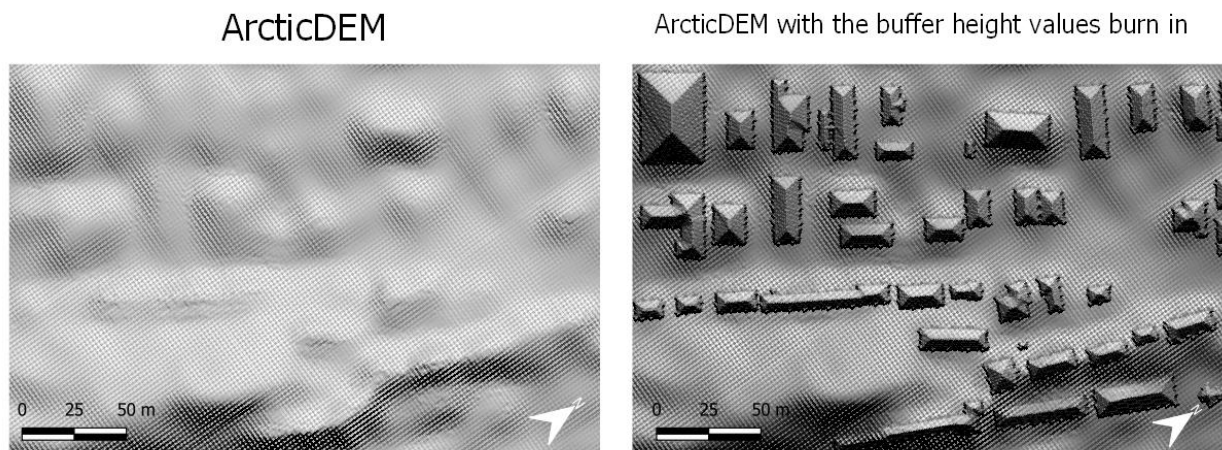


Figure 15 ArcticDEM before (left) and after (right) adding buffer height values from the vector layer.

3.2 Clear sky global solar irradiation modeling

Solar radiation model used in this master thesis is called r.sun¹² and is the package within the Geographical Resources Analysis Support System (GRASS)¹³. GRASS is a GIS platform started in 1982 by the U.S. Army Corps of Engineers Construction Engineering Research Laboratory (USA/CERL). It was created for the needs of the US military for environmental research, management, and monitoring of military sites. In the late 1990s, GRASS development was taken over by the State University of Illinois and University of Hanover. In October 1999, a new version of GRASS GIS was first published under the GNU General Public License and has since been distributed and developed as open-source software. (Neteler & Mitasova, 2008). The open-source philosophy of GRASS environment and QGIS application is one of the reasons why these products are chosen instead of the commercial alternative, which is Solar Radiation toolset available with ArcGIS Pro (distributed with Spatial Analyst license). GRASS was originally CLI oriented (Command Line Interface) environment. However continuous development and an increasing number of available modules and options was one of the reasons why in 1999 the first GUI (Graphic User Interface) for GRASS was created. (Landa, 2008)

The r.sun is a solar radiation model integrated with environment of the GRASS GIS. When calculating, it considers three components of solar irradiance/irradiation - beam, diffuse and reflected - both for clear-sky and for overcast conditions. All spatially differentiated variables can be provided to the model in a raster form, which makes r.sun an appropriate tool for modeling large areas. (Suri & Hofierka, 2004).

R.sun computes solar irradiance values in two modes. In mode 1 solar irradiance is calculated for the specific local time a solar incidence angle (degrees) and solar irradiance values (W/m^2). In Mode 2, which is used in this work, the model calculates the daily solar irradiation sum ($Wh/m^2/day$) for the selected day of the year.

Since calculating the insolation value for all 365 days of the year takes too much time and computing power, only the middle 12 days of each month were considered. One of the factors determining the amount of the solar energy that reaches a certain

¹² R.sun manual: <https://grass.osgeo.org/grass78/manuals/r.sun.html>

¹³ GRASS: <https://grass.osgeo.org/>

point on the Earth surface is the shape of the surrounding area. Shadowing effect has a particular impact on solar irradiance values in mountainous areas and where the relief is varied, such as the Greenland coast which is cut by fjords and surrounded by mountains and glaciers. To speed up the whole process of calculating solar irradiation potential first `r.horizon`¹⁴ module is applied to compute raster maps of the horizon height in a chosen direction. Step parameter in `r.horizon` module is set to 15 degrees and that generates 24 horizon maps for each location. Map starting with an angle 0 is showing horizon height towards East, next maps are changing directions every 15 azimuth degrees counterclockwise. The buffer zone parameter is set to 1500m, thanks to which the additional DEM area around the defined region is considered in the calculation of the horizon height. GRASS `R.slope.aspect` module is used to generate the slope and aspect maps. `R.latlong` module is applied to generate latitude and longitude raster maps. Horizon maps, slope and aspect maps, longitude, and latitude raster maps with elevation map are inputs data for the `r.sun` module.

Linke turbidity factor (TL) is a `r.sun` parameter that considers scattering and absorption by both the atmospheric gases and aerosol. (F.Kasten, 1996) As no data were found for Greenland cities and settlements, the model uses the average TL from other arctic locations, namely Utqiagvik (former Barrow) in the northern Alaska and Hornsund in Svalbard. (Remund, & Domeisen, 2010). TL value in the `r.sun` model is set to 2.5. Albedo value has a default value of 0.2. The output of the `r.sun` model is the irradiation raster map of the defined region containing sum of Wh on square meter in a set day of the year ($\text{Wh/m}^2/\text{day}$).

The GRASS GIS graphical modeler enable user to connect individual modules into a chain of processes. The use of the model accelerates and facilitates the performance of repetitive tasks. The model used in this thesis (Figure 16) has one variable. To run the model, user must enter the name of the chosen file containing raster DEM. The selected raster is automatically imported to the GRASS location, and its boundaries determine the default region for which all calculations are performed. In the next steps, the model generates latitude and longitude raster maps, slope, and aspect maps, and 24 horizon maps. This data serves as input to generate 12 solar

14 `R.horizon manual`: <https://grass.osgeo.org/grass78/manuals/r.horizon.html>

irradiation raster maps, which are exported to the selected folder. In the last step, all temporary raster files generated in the process are deleted.

GRASS model can be exported as python code, which allows sharing the model with other users¹⁵. The code contains paths to files and folders that need to be adapted before applying the model.

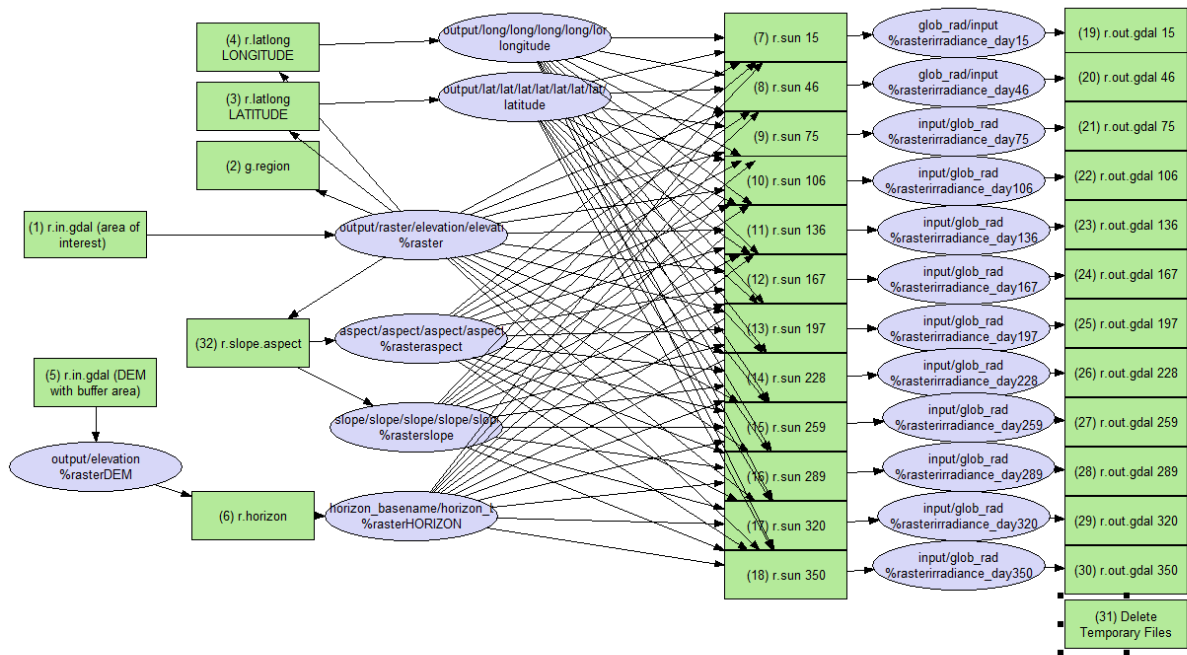


Figure 16 GRASS GIS graphical modeler

1416 solar irradiation maps were generated (12 maps for each of 118 locations, the files size 19,7GB). To facilitate further analysis of the results, raster maps showing the results for individual days were combined into single virtual raster (QGIS virtual raster tool).

Zonal statistic tool is applied to extract the mean value of global solar irradiation (Wh/m²/day) for each of the building outline. Mean value of global solar irradiation multiply by of the roof area in meters results in total number of the Wh of potential solar irradiation on the selected roof.

The sum of the rasters with results of solar irradiance potential for each month divided by 12, gives value of average day of the year.

¹⁵ GRASS model exported as a python script:
https://www.dropbox.com/s/bqxbi6ovxi3572f/irradiance_model.py?dl=0

4 Results

This chapter presents the results of the studies. The solar irradiation is computed for all the settlements in Greenland. 17787 polygons representing buildings footprints are used to extract the values from the solar irradiation raster maps. The output units produced by r.sun model is in the watt-hour per square meter per day ($\text{Wh}/\text{m}^2/\text{day}$). For easier reading of larger sums, watt-hours (Wh) will be converted into kilowatt-hours (kWh) megawatt-hours (MWh) or gigawatt-hours (GWh)¹⁶. All values presented in this chapter are the result of the clear-sky solar radiation model that does not consider the changing weather conditions such as cloudiness or snow cover.

The total solar irradiation potential on roofs in Greenland is estimated at 2,994¹⁷ GWh. As shown in the Figure 17, the size of the potential varies throughout the year. The highest value is recorded in June and equals 533,7 GWh, the lowest in December and equals 8,4 GWh. 84.8% of the potential solar irradiation is recorded during the half-year from the beginning of April to the end of the September.

Mean value of potential solar irradiation, for all roofs analyzed in the model in an average day of the year¹⁸ equals 2921 $\text{Wh}/\text{m}^2/\text{day}$. The mean solar irradiation is highest in June (6406 $\text{Wh}/\text{m}^2/\text{day}$), the lowest in December (85 $\text{Wh}/\text{m}^2/\text{day}$)(Figure 17). The highest mean value of solar global irradiation for a single building is 8649 $\text{Wh}/\text{m}^2/\text{day}$.

In winter, when the northern part of the island is plunged into the darkness of the polar night, there is no solar potential for electricity production. Starting from mid-November 1889 buildings north of 71.534°N are cut off from sunlight for 24 hours a day. In the middle of December, the polar night covers areas further south, and 9434 houses remain unreachable of the sun's rays. In January and February, 5704 and 420 buildings, respectively, are outside the reach of solar radiation. The potential solar irradiation for the four months from November to February is 127,4 GWh for all roofs in Greenland, which is 4.3% of the total annual potential.

¹⁶ 1 GWh = 1 000 MWh = 1 000 000 kWh = 1 000 000 000 Wh

¹⁷ Mean day of the month * number of the days in the month (sum of 12 months)

¹⁸ Average day of the year: Sum of rasters representing mean days of the month divided by 12

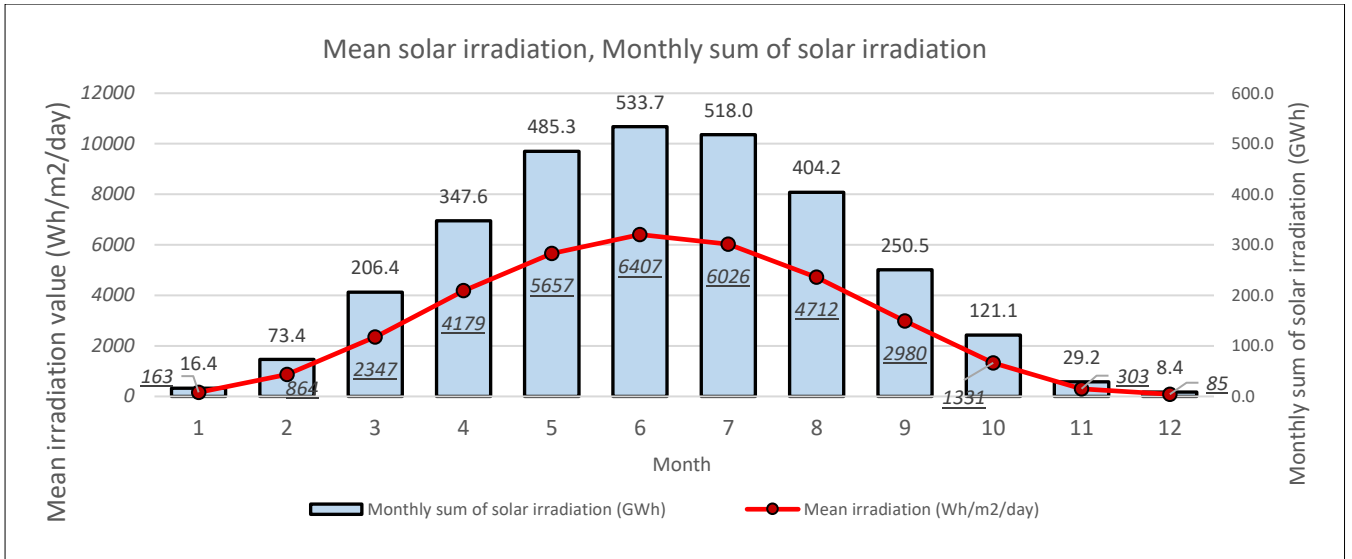


Figure 17 Monthly sum of solar irradiation and Mean irradiation value for an average day of the month

One of the variables affecting the results of the solar irradiation is latitude. As shown in the graph below (Figure 18), the tendency is that the results in the South are generally higher than in the North. This trend is particularly pronounced in the winter months when average values are at their lowest. From May to July, south of the 74°N

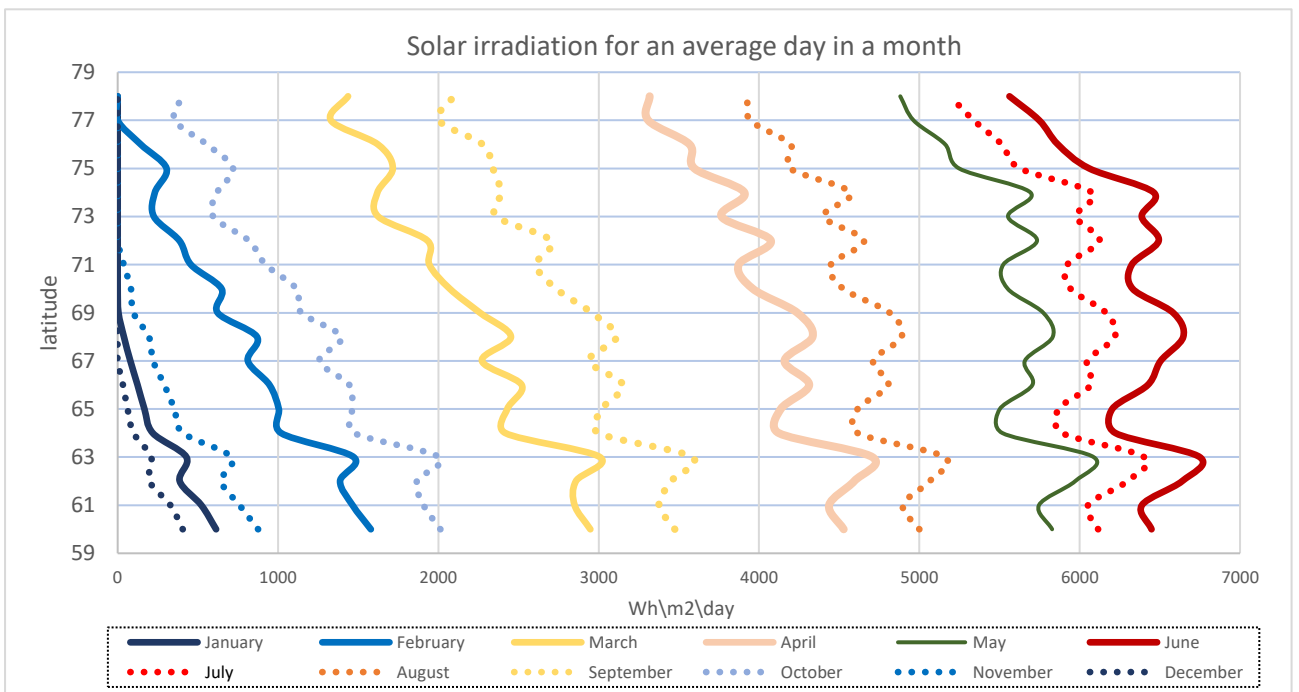


Figure 18 Solar irradiation for an average day in a month in relation to the latitude

parallel, the mean values do not decrease towards the north. The northernmost parts of the island (north of 74°N) have the lowest radiation values also in the summer months.(Figure 18).

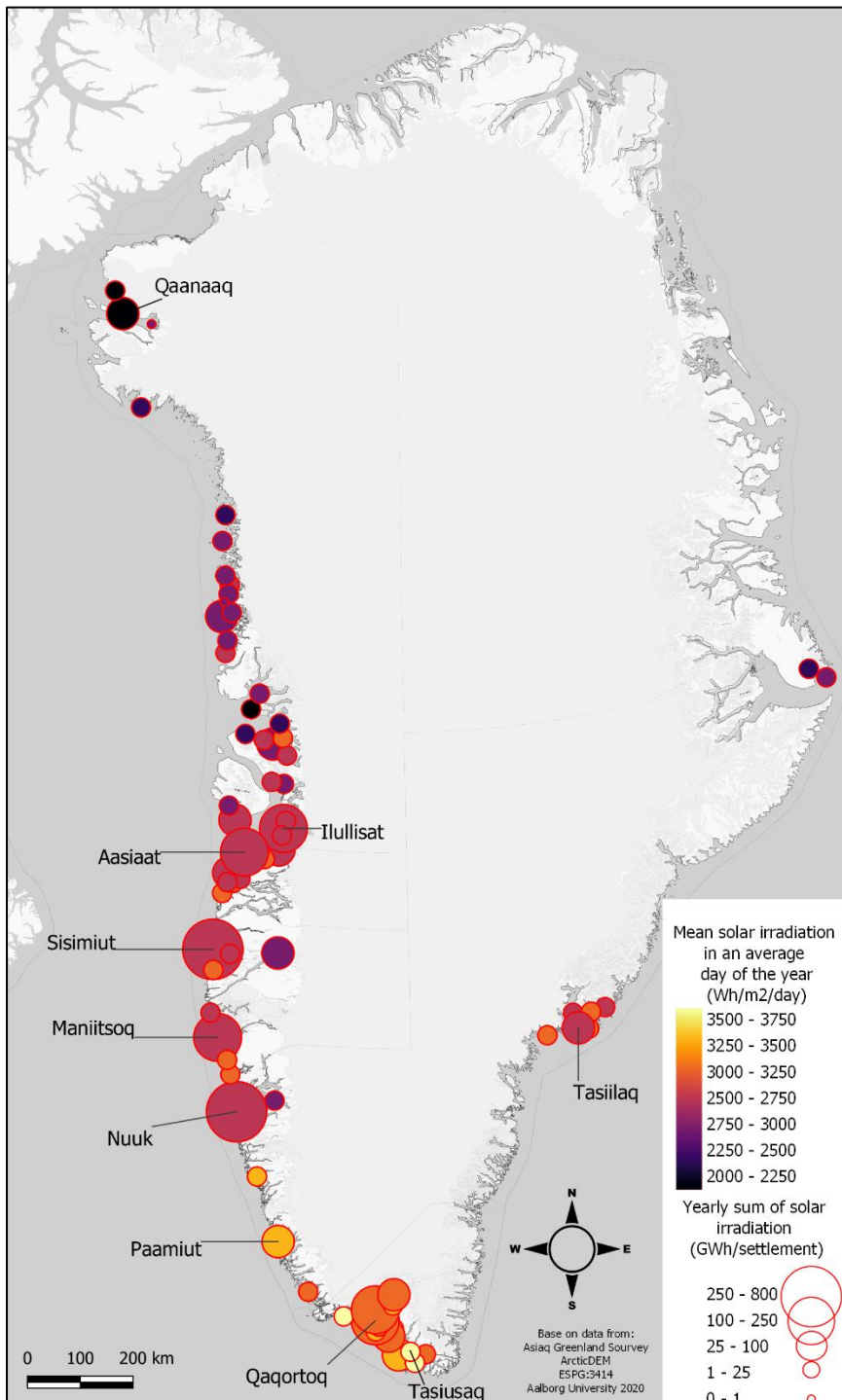


Figure 19 Greenland mean solar irradiation, potential Yearly sum of solar irradiation

solar irradiation in an average day of the year.

The size of the circles representing individual town or village corresponds to the yearly sum of solar irradiation. The yearly sum of potential solar irradiation for a

The relationship between the solar potential of roofs and latitude is also visible on the map on the left (Figure 19). Map presents mean solar irradiation values for an average day of the year group by the settlement. The further north of Greenland, the lower the values of the mean solar irradiation in an average day of the year. The values for separate localities are in the range from 2222 to 3670 Wh/m²/day. The lowest value is recorded for town of Qaanaaq (former Thule) located on 77°28'N. Tasiusaq 60°11'N is the settlement with the highest value of mean

particular town mainly depends on the sum of the roof areas in the location. Nuuk, the biggest town in Greenland has yearly potential of solar irradiation 749 GWh on its roofs, which is a quarter of the entire potential of the island.

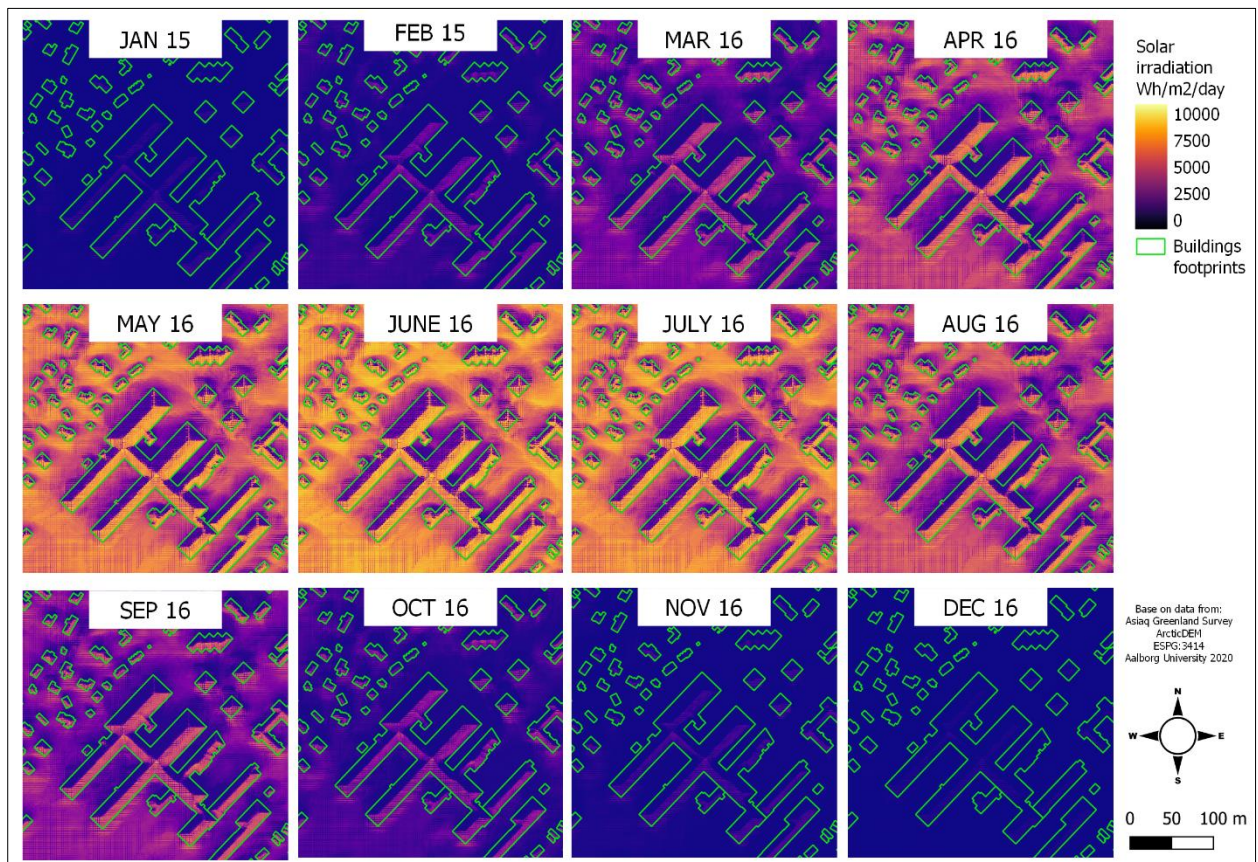


Figure 20 Solar irradiation in the middle day of the month. Example from Nuuk.

Figure 20 presents the results of solar irradiation for the middle days of the months. Above example from Nuuk shows the shapes of the modeled roofs and buildings footprints. The amount of potential solar irradiation differs depending on the part of the roof in which the values are measured. These differences are most visible in examples from the summer months when the irradiation values are highest. The south-facing roofs receive the highest amount of solar radiation, while the north-facing surfaces receive the least amount of solar energy. To analyze the impact of this dependency, raster with the irradiation values for the average day of the year is divided into four separated maps based on the slope direction. The individual pixels are assigned to the following groups:

- North-facing roofs - N - (315 > roof aspect <= 45)

- East-Facing Roofs - E - ($45 > \text{roof aspect} \leq 135$)
- South facing roofs - S - ($135 > \text{roof aspect} \leq 225$)
- West-Facing Roofs - W - ($225 > \text{roof aspect} \leq 315$)

Figure 21 presents a compilation of four rasters, each illustrates different roof slope direction. Pixels representing the selected aspect range are mapped in a color scale corresponding to the irradiation values, the rest of the pixels are shown in shades of gray. The average values of insolation for the roofs presented in the example are

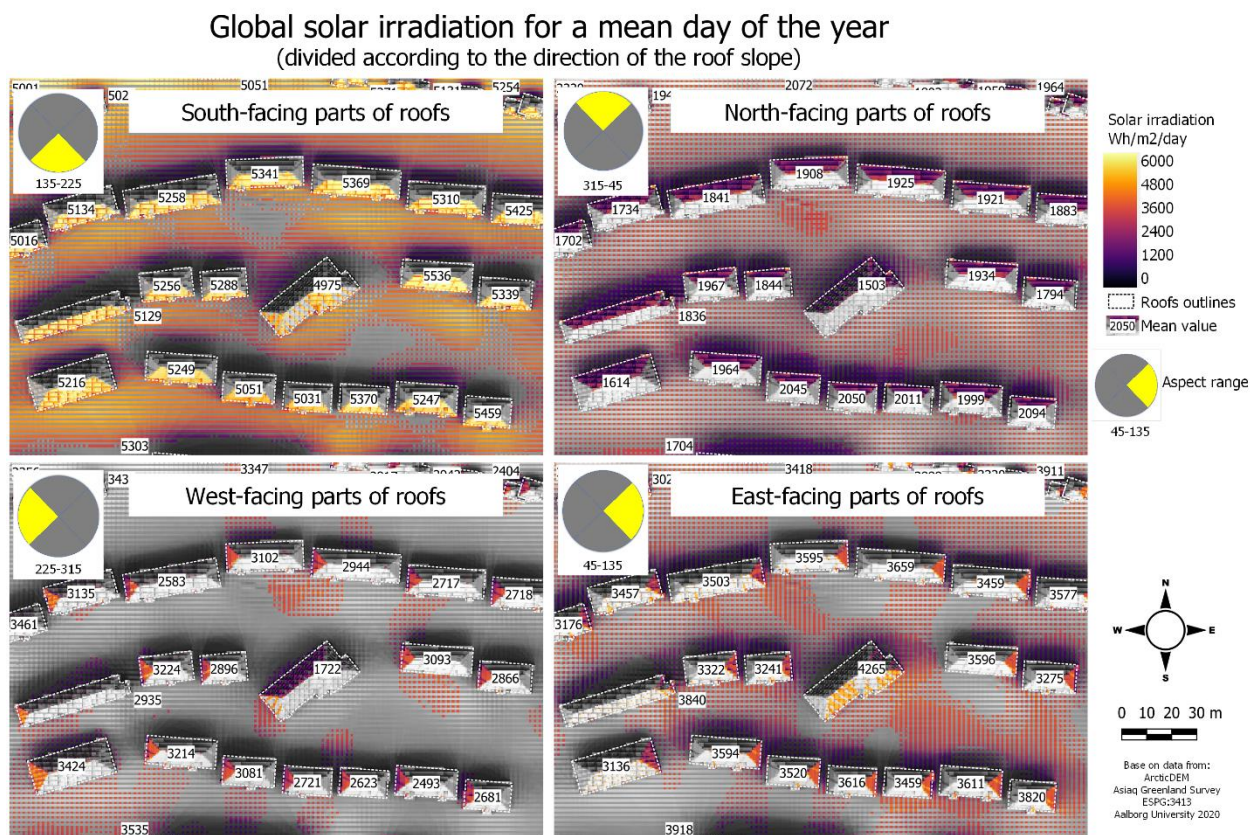


Figure 21 Mean solar irradiation in an average day of the year for four different roof slope directions

highest for pixels corresponding to the south facing parts of the roofs (aspect 135° to 225°). Most of the roofs in the south-facing example show the average insolation values above $5000 \text{ Wh/m}^2/\text{day}$. The lowest average values are on the second map with roofs facing north, and in most cases, do not exceed $2000 \text{ Wh/m}^2/\text{day}$. In most cases, the roofs facing east receive higher average solar irradiation than those facing west.

The mean values of solar irradiation for the average day of the year grouped by the aspect of the roof are shown in the graph in Figure 22. South-facing roofs have

the highest energy potential regardless of latitude. The highest values for this group of roofs are recorded in the south of Greenland, at 60°N mean value of solar irradiation equals 4810 Wh/m²/day. Values decrease towards north. In the northern part of the analyzed area at 78°N the average value is 2864 Wh/m²/day, which is a 40% less than in the southern part of Greenland. For north-facing roofs, the difference between mean values at 60°N and 78°N equals 20%. In an average day of the year, roof surfaces inclined towards the south, which covers 24% of the total roof area, generate 36% of the total solar energy. North inclined roof areas cover 28% of all roofs and have potential to produce 18% of energy in an average day of the year.

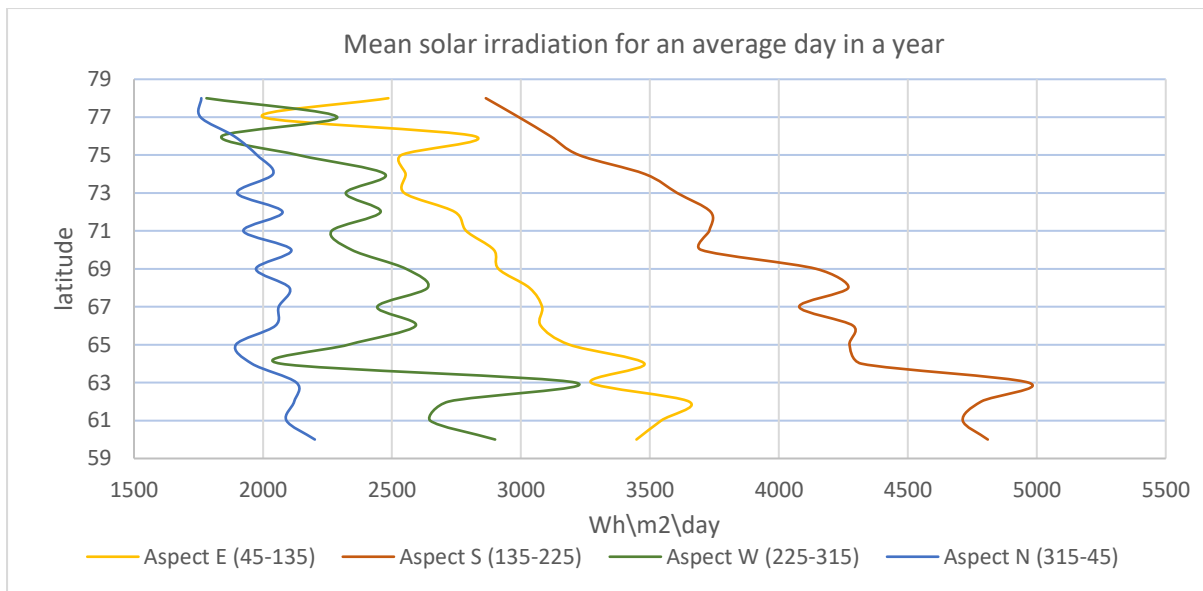
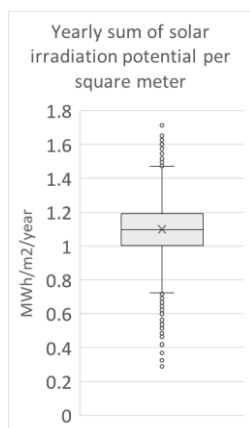


Figure 22 Mean solar irradiation for an average day in a year

Table 2 Solar irradiation values in an average day of the year grouped by roof aspect. (Buildings with flat roofs excluded)

Roof aspect	N (315-45)	E (45-135)	S (135-225)	W (225-315)
Solar irradiation (MWh)	1419	2038	2770	1484
Solar irradiation (%)	18	26	36	19
Area (m2)	756556	627168	645480	636959
Area (%)	28.4	23.5	24.2	23.9



Yearly sum of solar irradiation potential per m² range from 0,289 to 1,713 MWh/ m²/year. Mean value of yearly sum of potential solar irradiation from one square meter of roof in Greenland equals 1.099 MWh/m²/year. 50% of all values are within a range from 1.005 to 1.192 MWh/m²/year.(Figure 23)

Figure 23 Yearly sum of solar irradiation per m2

4.1 Data validation

Igaliku is a settlement in southern (61°N) Greenland. In 2017 energy company Nukissiofiit launched there the hybrid energy project consisting of 620m² of solar panels (100kW capacity), 68 wind turbines (20kW capacity), battery bank (190kW capacity) and two diesel generators (64kW capacity each) (Nymann Rud, et al., 2018). On its website¹⁹, Nukissiofiit publishes data on the volume of solar production in Igaliku in the period from January to September 2019.

Table 3 Comparison of electrical production from photovoltaic panels in Igaliku with the estimated solar irradiance potential. (*base on the mean solar irradiance potential for all the roofs in Igaliku in the mean day of the month) Source: Nukissiofiit and own results

	PV installation kWh monthly total production	PV installation kWh/m2 monthly production per square meter	PV installation Wh/m2/day daily production per square meter	Solar irradiance potential* Wh/m2/day daily potential per square meter	Daily production as % of potential solar irradiance
January	865	1.4	45	578.4	7.8%
February	1687	2.7	97	1530	6.4%
March	9326	15.0	485	2997	16.2%
April	8559	13.8	460	4699	9.8%
Maj	9835	15.9	512	6063	8.4%
June	13973	22.5	751	6695	11.2%
July	12471	20.1	649	6367	10.2%
August	10761	17.4	560	5199	10.8%
September	5904	9.5	317	3590	8.8%

¹⁹ https://www.nukissiofiit.gl/wp-content/uploads/2019/10/Igaliku_D.pdf

Table 3 presents the amount of electricity generated by photovoltaic system in Igaliku with the estimated solar irradiation potential values based on the average for all roofs in this settlement. On average, during the 9 analyzed months, electricity generated by photovoltaic panels accounted for 10% of the estimated solar irradiation potential. In March, electricity production from photovoltaics in Igaliku equals 16% of the estimated potential and it was the highest result. In February, 1687 kWh of produced energy equals 6.4% of the estimated potential and it is the lowest recorded ratio of these two values.

5 Discussion

The problem of global warming is one of the major challenges in the first half of the 21st century. The fight against the uncontrolled rise in temperature on Earth is one of the goals of the United Nations to lead to the sustainable development of humanity. Climate action - UN Goal number 13 - sets the task to take urgent action to combat climate change and its impacts²⁰. The Paris Agreement signed in 2016 by 196 countries assumes limiting the increase in global warming to below 2, and preferably to 1.5 degrees Celsius compared to the pre-industrial era (Rogelj, et al., 2016). One way to reduce greenhouse gas emissions, which are responsible for increasing the temperature of the atmosphere, is to reduce the combustion of fossil fuels (Lacis, Schmidt, Rind, & Ruedy, 2010). To meet the constantly growing energy needs of the world economy and at the same time reduce the consumption of coal, gas, and oil, it is necessary to increase the share of renewable energy sources in the total consumption. Declining production costs and increasing efficiency of photovoltaic panels make electricity obtained directly from the conversion of solar energy more accessible and its use economically viable. According to (Hosenuzzaman, et al., 2015) by 2030 use of photovoltaic systems can reduce emissions of 69–100 million tons of CO₂, 68,000–99,000 t of NO_x, and 126,000–184,000 t of SO₂.

To estimate the potential electricity production from a photovoltaic system, it is necessary to know its geographical potential. The solar irradiation value for a given point is the result of several factors such as latitude, day length and the height of the sun above the horizon depending on the season, shadows caused by the surrounding objects and terrain, air clarity, ground albedo value, weather conditions such as air temperature or cloud cover, and the angle and direction of inclination of the surface. The quality of the input data determines to what extent the modeled solar irradiation potential will match with the actual values.

²⁰ <https://sdgs.un.org/goals/goal13>

5.1 Limitations of the input data

In the process of estimating the solar irradiation potential of Greenland's roofs presented in this thesis, two main data sources are used:

- Raster maps with digital elevation model – ArcticDEM
- Vectors representing roof outlines

ArcticDEM is the most accurate public available free raster terrain model of Greenland. As shown in the previous chapters, the 2-meter resolution is enough to illustrate the terrain, but its accuracy does not reproduce the shapes of the roofs which are the subject of this study. Application of a higher resolution terrain model would increase the precision of mapping the terrain surface, at the same time multiplied number of pixels that must be analyzed, would significantly extend the computational time. The roof shapes are superimposed on the digital terrain model through the process described in the methodology chapter. The roof shapes generation method used in this thesis generates hipped roofs. Field observations and analysis of satellite images show that most houses in Greenland are covered with gable roofs. The analysis of the solar irradiation potential of roofs in Geneva presented by (Mohajeri, Assouline, Guibou, & Scartezzini, 2016) shows that the average annual sun irradiation on hipped roofs is 7.53% higher than on gable roofs. The difference in potential solar irradiation resulting from the type of roof was not considered in the results of this master's thesis.

Due to the low vegetation and the practical lack of trees in the arctic regions, the only factors shading the roofs in Greenlandic settlements are the neighboring buildings and the surrounding landforms, both represented in the converted ArcticDEM. It should be remembered that the roof model is only a simplification of the true shape of Greenlandic buildings. The buildings were divided into one and two-story groups. The shading influence of the higher buildings located in the centers of larger cities is not considered in this study. A buffer of 1500m is set around each of the regions for which the horizon maps are calculated. The effect of shading terrain forms and objects located more than 1500m from the analyzed area is not included in the calculations.

The simplifications of roof models are in part due to the limited amount of data contained in the vector layer containing the outlines of the buildings. The lack of information about the number of floors, height, type, and slope of the roofs prevented modeling a more realistic representation of the buildings.

5.2 Modeling process

One of the main variables influencing the amount of real-world solar irradiation not considered in the r.sun modeling process is cloud cover. All the results presented in the previous chapter are calculated for the clear sky conditions. Pfister et.al. (2003) shows in their research that there is high correlation between the mean reduction in surface irradiance values and the mean of the total cloud amount, with correlation coefficients of about -0.9 . As Lacour et al. (2017) presents in their article, the average observed cloud cover in Greenland in years 2008-2015 was 57%, with greater intensity in the southern part of the island 64%, and lower long-term average for the northern part that equals 53%. The cloudiness undoubtedly increase the difference between the solar irradiation potential of roofs and the real amounts of energy that can be produced on the analyzed roof surface.

Snow is another factor that reduces the ability of utilization of solar irradiation potential. Snow-covered solar panels do not produce electricity. The experiment described by Pawluk et al. (2019) shows that solar panels covered with snow had an annual electricity production of between 6% and 26% lower than an adjacent panels that were cleaned from snow cover. In the same paper, the authors conclude that snow cover on solar panels typically accounts for the loss of 10% of potential electrical production. It should be borne in mind that the results presented by Pawluk et al. (2019) are based on data from locations in Canada, the USA, Germany and Japan, places at lower latitudes than most of Greenland.

Lack of freely available high-resolution raster maps containing the ground albedo value for the coast of Greenland did not allow for thorough consideration of this factor in the calculations. Solar irradiation potential is estimated using the default albedo coefficient 0.2. To check the impact of the albedo factor on modelled solar irradiation, a 270×390 m raster representing part of Nuuk containing 31 buildings was tested. The insolation for an average day of the year was calculated using the following

albedo values: 0; 0.1; 0.2; 0.4; 0.8 and 1. Increasing the albedo parameter from the default 0.2 to 0.4 results in an increase in the insolation value for the average day of the year for the examined buildings by 1.9%, increasing the albedo to 0.8 and to 1 causes an increase by 6,7% and 8.9%. The reduction of the albedo parameter from 0.2 to 0.1 and to 0 resulted in a decrease in the solar irradiation value on the average day of the year by -2% and -3.4%, respectively. The relatively small influence of the albedo coefficient on the final results can be explained by the low proportion of reflected radiation in the global radiation.

Settlements scattered along the coast of Greenland extend between southern and northern part of the island on over 2000 km. The results presented in chapter reflect the latitudinal extension of the island. The northernmost regions are characterized by a lower solar radiation potential, the further south, the higher the values. In addition to the general differentiation resulting from the latitude, there are also local differences between the neighboring settlements, which result from the terrain relief conditions and the roof characteristics. In addition to spatial variation, the results show significant temporal variation. Low, and sometimes zero solar potential during winter makes it impossible to make solar radiation in Greenland the only source of energy. Analysis of individual buildings indicates that, the greatest potential for generating electricity have roofs inclined towards the south, the next in the order are those directed to the east.

The amount of electricity generated by the photovoltaic system installed in Igaliku, per square meter is on average ten times lower than the solar irradiation potential modeled for the roofs in this settlement. One of the main reasons for such a difference between the geographical potential insolation, and the actual energy production, is the efficiency of photovoltaic systems (technical potential). The efficiency of photovoltaic panels is the ratio of the amount of solar energy reaching the panels surface to the amount of electricity that is generated from received solar energy. (Shubbak, 2019) The yield of the most popular silicon photovoltaic panels is about 20%. After considering the efficiency of the panels, the modeled solar irradiation value for Igaliku roofs is twice as high as the real production of the photovoltaic system. This difference can be explained by the weather conditions prevailing on the island. As mentioned above, the annual cloud cover is over 50%, the snow cover also reduces the possibility of the full use of solar energy potential.

Data from Igaliku (Table 3) show that although the amount of electricity produced per square meter of photovoltaic panels is approximately 10% of the modeled geographical clear sky solar potential, the use of solar energy gives considerable savings. Between January and September 2019, the share of solar energy in total energy consumption in Igaliku ranged from 4.1% in January to 93.8% in June, the average share was 46.4%. The reduced demand for the energy produced by a diesel generator allowed to save 17,100 liters of petroleum fuels in this period.²¹

5.3 Future work

This section will consider how more detailed results can be obtained and how the project could continue could be developed in future.

One possible scenario when using the same input data, would be to change some model parameters to achieve more precise results:

- increasing the buffers size around the studied area of interest to produce more detailed horizon maps
- increasing the number of horizon maps used to simulate the shading effect
- smaller intervals between days for which insolation is calculated

All listed above changes in the model settings would result in an extended calculation time. In the case of calculations for an increased number of days for which calculations are performed, a larger amount of storage would be required. Another way to increase the accuracy of the results would be the use of data from other sources:

- high resolution Digital Surface Model based on lidar data – the terrain model based on data collected using lidar is characterized by relatively high detail. Resolution of several centimeters exactly maps the terrain and shapes of buildings. The initial plan was to use this type of data to calculate solar irradiation. Unfortunately, the lidar data DSM that was made for the five largest cities in Greenland was not published until this master thesis was completed. (GIM, 2020)

²¹ https://www.nukissiorfiit.gl/wp-content/uploads/2019/10/Igaliku_D.pdf

- high resolution albedo raster map instead of single coefficient value
- use high resolution Linke atmospheric turbidity coefficient input raster map instead of a single value

More data about electricity production from existing in Greenland solar PV installations is necessary to better understand how solar irradiation potential translates into the amount of produced electricity.

Publication of the results on the Web GIS platform (e.g., using ArcGIS Online) will enable an accessible way of presenting data to a mass audience. The presentation of the results in the form of an interactive map, similar like in Google Project Sunroof²², should allow the user to assess the potential of the photovoltaic installation on the roof of the selected building.

²² <https://www.google.com/get/sunroof>

6 Conclusion

The aim of this thesis is to create solar irradiation potential estimation for rooftops in country of Greenland. The use of open-source data and technologies allowed for low-cost estimation of the geographical solar potential for each building in the research area. A dataset of buildings in which each of the objects has the attribute of the amount of solar irradiation per square meter per day (Wh / m² / day) is created. Based on the roof area and average insolation values, the sums of solar irradiation potential for the roofs were also calculated. The average values of the insolation of the roofs were calculated for the middle day of each month.

2-meter resolution terrain model that is being used in this work, reproduces buildings shapes only to the limited extent. Modifications to the raster maps with the terrain model were necessary to obtain a better representation of the roof shapes. A vector layer with attributes specifying the angle of inclination and the height of the roof was used to modify the elevation model. Modifications have improved the precision of the roof shapes representation in ArcticDEM. The roof parameters used to modify the terrain model are the result of field observations and satellite image analysis, and therefore do not fully correspond to the real picture of buildings in Greenland. The improved terrain model should not be viewed as an accurate representation of reality. ArcticDEM can be the basis for generating a sufficiently detailed model of buildings, which latter may be used in modeling the rooftop solar irradiation.

The results show a significant temporal and spatial variation in the solar irradiation potential of roofs in Greenland. The obtained values indicate a high solar potential in the summer and low, in some regions equal to zero, during the winter months. In the south of Greenland, the solar irradiation potential of roofs is higher than in the north. There are local exceptions to this pattern due to environmental conditions, such as shading caused by the topography. The differentiation of the insolation intensity is also visible on the scale of individual buildings, parts of roofs inclined towards the south are characterized by the highest solar irradiation potential.

Bibliography

- Asiaq Greenland Survey. (n.d.). *Asiaq*. Retrieved from Product description: Asiaq's Basemap: https://kortforsyning.asiaq.gl/Downloads/EN_Product_Description_Basemap.pdf
- F.Kasten. (1996). The linke turbidity factor based on improved values of the integral Rayleigh optical thickness. *Solar Energy*, 56(3), 239-244.
- Fu, P., & Rich, P. (1999). Design and implementation of the Solar Analyst: an ArcView extension for modeling solar radiation at landscape scales. *Proceedings of the Nineteenth Annual ESRI User Conference*. Retrieved from https://www.researchgate.net/profile/Paul-Rich/publication/266576778_Design_and_implementation_of_the_Solar_Analyst_an_ArcView_extension_for_modeling_solar_radiation_at_landscape_scales/links/54cd75d20cf29ca810f839ea/Design-and-implementation-of-the-Solar
- GIM. (2020, 01 29). *Using Lidar North of the Arctic Circle*. Retrieved from GIM International: <https://www.gim-international.com/content/article/using-lidar-north-of-the-arctic-circle>
- Google. (2017). *Project Sunroof data explorer: a description of methodology and inputs*. Retrieved from <https://static.googleusercontent.com/media/www.google.com/en//get/sunroof/assets/data-explorer-methodology.pdf>
- Greenland, S. (2020). *Statistics Greenland*. Retrieved from Population: <http://www.stat.gl/dialog/topmain.asp?lang=en&subject=Population&sc=BE>
- Hetrick, W. A., Rich, P. M., & Weiss, S. B. (1993). Modeling insolation on complex surfaces. *Thirteenth Annual ESRI User Conference*, 2, pp. 447–458. Retrieved from http://professorpaul.com/publications/hetrick_et_al_1993_esri.pdf
- Hofierka, J., & Kaňuk, J. (2009). Assessment of photovoltaic potential in urban areas using open-source solar radiation tools,. *Renewable Energy*, 34(10), 2206-2214. doi:<https://doi.org/10.1016/j.renene.2009.02.021>.
- Hofierka, J., & Zlocha, M. (2012, October). A New 3-D Solar Radiation Model for 3-D City Models. *Transactions in GIS*, 681-690. doi:<https://doi.org/10.1111/j.1467-9671.2012.01337.x>
- Hoogwijk, M. M. (2004). On the global and regional potential of renewable energy sources. *Doctoral Research*. University of Utrecht. Retrieved from <https://dspace.library.uu.nl/bitstream/handle/1874/782/full.pdf?sequence=1&isAllowed=y>
- Hosenuzzaman, M., Rahim, N., Selvaraj, J., Hasanuzzaman, M., Malek, A., & Nahar, A. (2015). Global prospects, progress, policies, and environmental impact of solar photovoltaic power generation. *Renewable and Sustainable Energy Reviews*, 41, 284-297.
- Kumar, L., Skidmore, A. K., & Knowles, E. (1997). Modelling topographic variation in solar radiation in a GIS environment. *International Journal of Geographical Information Science*, 10(5), 475-497. doi:10.1080/136588197242266
- Lacis, A. A., Schmidt, G. A., Rind, D., & Ruedy, R. A. (2010). Atmospheric CO₂: Principal Control Knob Governing Earth's Temperature. *Science*, 330, 356-359. Retrieved from <http://www.jstor.org/stable/40931614>
- Lacour, A., Chepfer, H., Shupe, M. D., Miller, N. B., Noel, V., Kay, J., . . . Guzman, R. (2017). Greenland Clouds Observed in CALIPSO-GOCCP: Comparison with Ground-Based Summit Observations,. *Journal of Climate*, 30(15), 6065-6083. doi:<https://doi.org/10.1175/JCLI-D-16-0552.1>
- Lading, T. (2015). *Barriers and drivers for energy efficient homes in Greenland*. Lyngby: DTU BYG / Center for Arctic Technology.
- Landa, M. (2008). New GUI for GRASS GIS based on wxPython.

- Mohajeri, N., Assouline, D., Guibou, B., & Scartezzini, J. L. (2016). Does roof matter? Solar PV integration on roofs. *Expanding Boundaries: Systems Thinking in the Built Environment: Sustainable Built Environment (SBE)* (pp. 130-135). Zurich: vdf Hochschulverlag AG.
- Morin, P., Porter, C., Howat, I., Noh, M.-J., Willis, M., Bates, B., . . . Peterman, K. (2016). ArcticDEM; A Publically Available, High Resolution Elevation Model of the Arctic. *EGU General Assembly Conference Abstracts*. Retrieved from <https://ui.adsabs.harvard.edu/abs/2016EGUGA..18.8396M>
- Neteler, M., & Mitasova, H. (2008). *Open Source GIS : A GRASS GIS Approach* (3rd ed.). New York, NY, USA: Springer Science.
- Nymann Rud, J., Hormann, M., Hammervold, V., Asmundsson, R., Georgiev, I., Brondum, S., . . . Brodsted, M. R. (2018). *Energy in the West Nordics and the Arctic: Case Studies*. Copenhagen: Nordic Council of Ministers/Publication Unit.
- Pawluk, R. E., Chen, Y., & She, Y. (2019). Photovoltaic electricity generation loss due to snow – A literature review on influence factors, estimation, and mitigation,. *Renewable and Sustainable Energy Reviews*, 107, 171-182. doi:<https://doi.org/10.1016/j.rser.2018.12.031>.
- Pfister, G., McKenzie, R. L., Liley, J. B., Thomas, A., Forgan, B. W., & Long, C. N. (2003, 10 01). Cloud Coverage Based on All-Sky Imaging and Its Impact on Surface Solar Irradiance. *Journal of Applied Meteorology*, 42(10), 1421-1434. doi:[https://doi.org/10.1175/1520-0450\(2003\)042<1421:CCBOAI>2.0.CO;2](https://doi.org/10.1175/1520-0450(2003)042<1421:CCBOAI>2.0.CO;2)
- Remund, J., & Domeisen, D. (2010). *Aerosol optical depth and Linke turbidity climatology*. Bern: Genossenschaft METEOTEST.
- Rogelj, J., den Elzen, M., Höhne, N., Fransen, T., Fekete, H., Winkler, H., . . . Meinshausen, M. (2016, June 29). Paris Agreement climate proposals need a boost to keep warming well below 2 °C. *Nature*, 631–639. doi:<https://doi.org/10.1038/nature18307>
- Scharmer, K., & Grief, J. (2000). *The European solar radiation atlas: Fundamentals and maps* (Vol. 1). Paris, France: Les Presses de l'École des Mines.
- Shubbak, M. H. (2019). Advances in solar photovoltaics: Technology review and patent trends. *Renewable and Sustainable Energy Reviews*, 115. doi:<https://doi.org/10.1016/j.rser.2019.109383>.
- Suri, M., & Hofierka, J. (2004, April 1). A New GIS-based Solar Radiation Model and Its Application to Photovoltaic Assessments. *Transactions in GIS*, 8(2), 175-190.
- Suri, M., Huld, T. A., & Dunlop, E. D. (2005). PV-GIS: a web-based solar radiation database for the calculation of PV potential in Europe. *International Journal of Sustainable Energy*, 24(2), 55-67. doi:10.1080/14786450512331329556